Desalination and Water Treatment
www.deswater.com

doi: 10.5004/dwt.2019.23573

150 (2019) 105–113
May

Lead removal from water using DES functionalized CNTs: ANN modeling approach

Seef Saadi Fiyadh[a], Mohammed Abdulhakim AlSaadi[a,b,*], Mohamed Khalid AlOmar[c], Sabah Saadi Fayaed[c], Ahmed El-Shafie[d]

[a]*Nanotechnology & Catalysis Research Centre (NANOCAT), IPS Building, University of Malaya, 50603 Kuala Lumpur, Malaysia, Tel. +60163630693; Fax: +6037967 5311; emails: mdsd68j@gmail.com (M.A, AlSaadi), Saadisaif3@gmail.com (S.S. Fiyadh)*
[b]*National Chair of Materials Science and Metallurgy, University of Nizwz, Sultanate of Oman, Nizwa, Oman*
[c]*Department of Civil Engineering, Al-Maaref University College, Ramadi, Iraq, emails: mohd.alomar@yahoo.com (M.K. AlOmar), Sabahal_fayath2006@yahoo.com (S.S. Fayaed)*
[d]*Department of Civil Engineering, University of Malaya, Kuala Lumpur 50603, Malaysia, Tel. +60122003857; email: elshafie@um.edu.my*

Received 23 June 2018; Accepted 6 December 2018

ABSTRACT

The removal of lead ions from water is investigated in this study, the non-linearity relationship between the parameters used in the adsorption process were modeled. The artificial neural network modeling method has been used to reflect the non-linear relationship between the variables of the process. A novel functionalized carbon nanotube is used to adsorb Pb(II) ions from water. A total of 158 runs were performed at a laboratory scale and used for modeling. The adaptive neuro fuzzy inference system (ANFIS) model more accurately described the adsorption process, the ANFIS R^2 was 0.998, and a feed-forward neural network (FF-NN) R^2 was 0.993. Various indicators were used to determine the model's efficiency and accuracy. To classify the adsorption kinetic order, three kinetic models were evaluated. The pseudo-second-order model was well fitted to the simulated data. The maximum relative error was 7.078% for the ANFIS model and 11.62% for the FF-NN, indicating the higher accuracy of the ANFIS model.

Keywords: Carbon nanotubes; Lead removal; Water treatment; Deep eutectic solvent; Neural network

1. Introduction

The need for fresh water is highly important for life. Researchers have reported that heavy metal ions, such as Pb(II), As(III), Cr(III) and Cd(II), have deleterious effects on human life. Heavy metal ions arrive in water resources in different ways from various industries. Several heavy metal ions are poisonous even at low concentrations and can cause harm if they accumulate in a living organism [1]. Lead elements are typically found in small quantities in the earth's upper layer. Lead generates a variety of diseases and disorders in the human body. Therefore, environmental protection agencies and researchers worldwide are engaged in treating water to remove these ions. The World Health Organization recommends 0.01 μg/L as the maximum allowable limit of lead in drinking water [2]. The allowable lead ion concentration in industrial wastewater is 3.0 μg/L [3]. Various remediation methods have been used to remove heavy metals from aqueous solution, including precipitation [4], reverse osmosis [5], coagulation [6], oxidation [7], ion exchange [8] and adsorption. Moreover, the heavy metals are available in soil, different methods were used to remove the heavy metals from soil [9–11]. The adsorption process has advanced in terms of design simplicity, operation and cost. The effectiveness

* Corresponding author.

of adsorption primarily depends on the selection of an appropriate processing condition, including the mass of sorbent, pH, system temperature and process duration [12].

Many studies have been performed using various materials as adsorbents to extract metal cations, such as activated carbon [13], clay minerals [14], biomaterials [15] and pistachio shells [16]. However, these adsorbents have proven unsatisfactory. Researchers have proposed carbon nanotubes (CNTs) as the most effective adsorbents for removing numerous pollutants. Their large surface area and diameter and their shorter equilibrium time compared with other materials contribute to their effective application [17]. The CNTs have been successfully used to extract various heavy metals, for instance chromium, copper, zinc, lead, cadmium, arsenic and mercury [18]. However, functionalization is the key to improving the capability of CNTs. Conventional functionalization typically involves harsh acids, non-environmentally friendly chemicals and complicated processes. Thus, the need for environmentally friendly functionalization agents with simple chemical processes is crucial [19].

Recently, deep eutectic solvents (DESs) have received substantial research interest because of their wide applicability. The DESs are one of the ionic liquid (IL) analogues which are presented by Abbot et al. [20] as a cheaper replacement for developed ILs. DESs were first introduced as a low-cost means to replace ILs. DESs have many advantages over ILs in terms of the availability of the raw materials and their ease of synthesis with minimal environmentally harmful waste [21]. Therefore, DESs have been adopted in many areas of science. Recently, DESs have been used in several nanotechnology fields as a medium for nanoparticle synthesis, as electrolytes in nanostructure sensors, as electrolytes in nanoparticle deposition [22] and as CNT functionalization agents [19,23]. AlOmar et al. [25] used choline chloride-based DESs as novel CNT functionalization agents to prepare a sufficient adsorbent of Pb(II) ions. DESs generally consist mainly of hydrogen bond donor (HBD) and salt, both compounds are in solid form at room temperature whereby, their mixture gets converted into liquid phase. The melting point of the mixture is less than the average melting points of the individual compounds [24]. In contrast, DES has several advantages comparing with the conventional ILs such as diversity of physical properties and different molar ratios and cheaper price of compounds.

The adsorption process is complicated due to the non-linear relationship of the involved variables to the adsorption capacity of CNTs. Modeling this type of process is complex when using linear correlation methods. The artificial neural network (ANN) represents an alternative modeling method. ANN is a powerful tool for recognizing the relationships between the inputs and outputs using training process. Because of the expense of the CNTs used in the experiments and the complicated process of preparing the experiments, the ANN modeling method is useful for formulating knowledge, describing the process and extending experimental results. Scaling up from the research facility to the industrial level is simpler when process models are used. In contrast, heuristic models are recommended for collecting information without performing additional experimental research. These kinds of models are designed to recognize the complex, non-linear relationships between variables and are easier to use.

This study aims to develop useful applicable model using the proposed artificial network system, a feed-forward neural network (FF-NN) and the adaptive neuro fuzzy inference system (ANFIS) to predict Pb(II) ion removal from water using DES-functionalized CNTs and a set of experimental data prepared at a laboratory scale. The performance and efficacy of the FF-NN model are compared with those of the ANFIS model. The sensitivity study of the involved parameters is examined in this research. Three kinetic models are applied to the predicted results to assess the rate of the adsorption reaction.

2. Experiment setup

2.1. Experimental

In a previous study, a novel Pb(II) adsorbent was prepared based on pristine CNTs oxidized with $KMnO_4$ and then functionalized by choline chloride: triethylene glycol (salt:HBD) 1:2 DES (TEG) [25]. The preparation of the adsorbent was performed in two stages. The primary oxidation involved sonication of pristine-CNTs (P-CNTs) with $KMnO_4$ for 2 h at 65°C, the pristine-CNTs (P-CNTs) are provided from Sigma-Aldrich (Malaysia). Subsequently, the resulting oxidized CNTs (K-CNTs) were sonicated with DES for 3 h at 65°C to produce KTEG-CNTs. The adsorbent was comprehensively characterized by observing the Raman shift using Raman spectroscopy. The functional groups associated with the functionalization process were analyzed using FT-IR. The surface charge, surface area and surface morphology were investigated using the zeta potential, BET surface area field-emission scanning electron microscope and TEM, respectively. The structural phase was also investigated by conducting an XRD profile. The characterization results had been presented in our previous publications [25]. Additionally, a batch adsorption study was performed at an ambient condition. The adsorption capacity of KTEG-CNTs was understood as a response to four variables: initial concentration, adsorbent dosage, pH value and contact time. A total of 158 experimental results based on different conditions were used to study the influence of each parameter on the adsorption capacity and the interaction among the parameters. The restrictions for each parameter are listed in Table 1.

2.2. Artificial neural network

The artificial neural network (ANN) has been considered a less complicated model of sophisticated biological networks. As an alternative modeling technique, artificial neural network (ANN) has been used to represent the non-linear

Table 1
Evaluation indicators

	ANFIS	FF-NN
MSE	6.14×10^{-5}	1.86×10^{-4}
RMSE	6.47×10^{-3}	1.36×10^{-2}
RRMSE	5.91×10^{-3}	5.74×10^{-2}
MAPE	2.02	4.53

function relationship among variables. The ANN techniques do not require mathematical induction since the ANN analyzes examples and recognizes patterns in a series of inputs and outputs of a dataset without prior assumptions regarding their characteristics and interrelations [26]. The special ability of ANN to generalize and identify the pattern of any non-linear, complex development makes it an influential modeling tool. Neural networks can extract complicated data that cannot be observed by a human or a computer technique. Several studies have recently been conducted on water quality prediction models [27]. Additionally, research has been performed on, for example, modeling fermentation media optimization and modeling a microwave-assisted extraction method.

A feed-forward back-propagation neural network (FF-NN) was used in this study as a gradient descent technique to minimize network error. Each layer in the FF-NN has several neurons, and each neuron transmits input values and processes to the next layer. As illustrated in Fig. 1, the value of the input variable is multiplied by the connection weights w_{ii}, which connect the input to the hidden layer. The FF-NN model consists of input layers, hidden layers and one output layer in a multilayer neural network.

Because the FF-NN is a supervisory learning algorithm technique, the method used to select the optimal parameters is to adjust the network weight value [28]. The term "Optimal" refers to the difference between target values or actual values t_k and the network output z_k that achieves the minimum or the target such that

$$E = \frac{1}{2}\sum_{k=1}^{k}(z_k - t_k)^2 \quad (1)$$

Here, z_k = ANN output, and t_k is the target output T. The training process is a procedure whereby the ANN connecting weights are modified by a continuous procedure of stimulation on the condition that the network is fixed.

The input data are normalized in a range of 0–1 to avoid over-fitting the network. It is realized that all the units of a similar layer do not connect with one another. The connections among the developed layers can be expressed by the coefficient of weight [29].

The weighted signals and bias from the input neurons are summed by the hidden neurons and then projected through the transfer function. In the FF-NN algorithm, the inputs are forwarded into the network until the end of the network. The output is initiated and compared with the target value. Finally, the error is calculated.

Back-propagation learning is used to create the relationship between the target outputs and the input data, which are typically assigned with a random initial weight and later updated by comparing the results of the actual values with the target values. In the diverse research that uses neural computations, different transfer functions are used depending on the problem non-linearity and data complexity to design a proper network.

2.3. ANFIS architecture and development

The adaptive neuro fuzzy inference system (ANFIS) technique is a feed-forward multilayer network that uses fuzzy logic and a neural network learning system to format the input data space to the output data space. The ANFIS learning system consists of five layers. Each layer consists of several nodes.

There are two types of fuzzy inference systems (FISs): the Mamdani and Assilian type [30] and the Takagi and Sugeno type [31]. The consequence parameter definition is an important difference between the two FISs. The results parameter in the Sugeno FIS is either a constant coefficient [32] (i.e., the zero-order Sugeno FIS) or a linear equation (i.e., the first-order Sugeno FIS).

The procedures of the ANFIS can be summarized to assist comprehension. It is considered that the system contains four inputs, that is, contact time (T), concentration of Pb(II) (C), pH (PH) and adsorbent dosage (AD), and one output removal efficiency (Q). The rule base consists of four fuzzy if-then rules. The four rules can be written as follows:

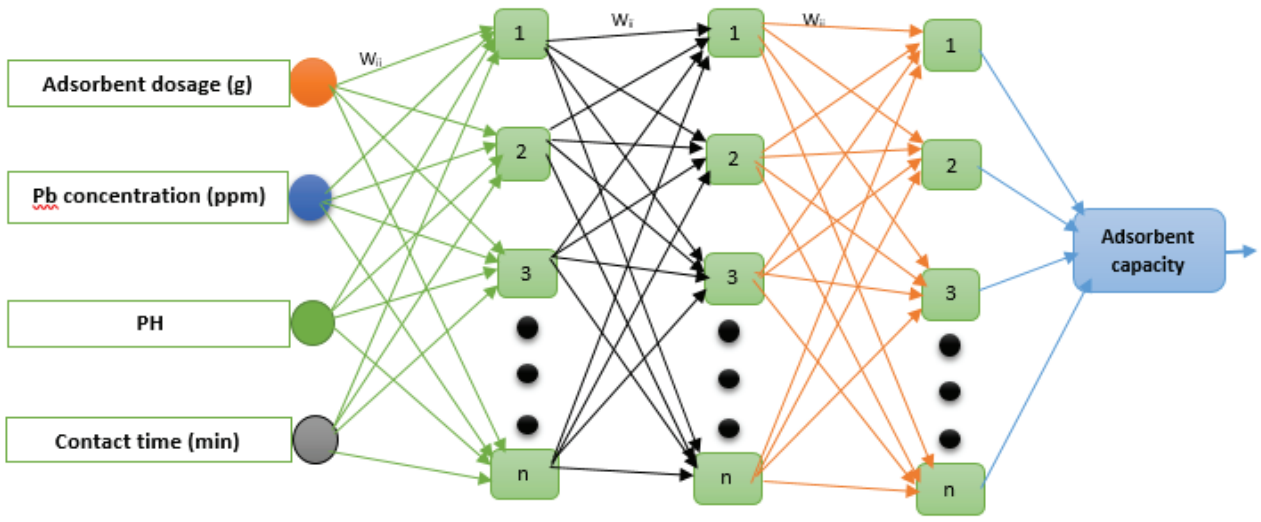

Fig. 1. Feed-forward back-propagation neural network structure.

Rule 1:

If AD is A_1, C is B_1, PH is C_1 and T is D_1, then $f_1 = p_1 \times \text{AD} + q_1 \times C + s_1 \times \text{PH} + m_1 \times T + g_1$

Rule 2:

If AD is A2, C is B_2, PH is C_2 and T is D_2, then $f_2 = p_2 \times \text{AD} + q_2 \times C + s_2 \times \text{PH} + m_2 \times T + g_2$

where q_i, p_i, s_i, m_i and g_i ($i = 1, 2, 3,\ldots$) are considered the linear parameters in the consequential part of the Sugeno fuzzy system. The ANFIS constriction is illustrated in Fig. 2, and the ANFIS model description is as follows:

Layer 1: the input node. The input node of the first layer produces the membership grades for the input and output O_{i1}, which is calculated by the following:

$$O_{i1} = \mu A_i(\text{AD}) \qquad (i = 1, 2) \tag{2}$$

$$O_{i1} = \mu B_{i-2}(C) \qquad (i = 3, 4) \tag{3}$$

$$O_{i1} = \mu C_{i-4}(\text{pH}) \qquad (i = 5, 6) \tag{4}$$

$$O_{i1} = \mu D_{i-6}(T) \qquad (i = 7, 8) \tag{5}$$

where AD, C, pH and T are the inputs to node I, and A_i, B_i, C_i and D_i are the linguistic labels categorized by the appropriate membership functions (MFs) μA_i, μB_i, μC_i and μD_i, respectively.

Layer 2: the node rules. The layer outputs, termed firing strengths O_{i2}, are the corresponding degrees transferred from the previous layer output (Layer 1).

$$O_{i2} = w_i = \mu A_i(\text{AD})\mu B_i(C)\ \mu C_i(\text{pH})\ \mu D_i(T), \qquad (i = 1, 2, 3\ldots.) \tag{6}$$

Layer 3: the nodes average. The purpose of the third layer is to compute the ratios of all the ith rules' firing strengths to sum the firing strength of the rules. Accordingly, $\bar{w}_i$ is considered a regularized firing strength.

$$O_{i3} = \bar{w} = \frac{w_i}{\sum_i w_i} \tag{7}$$

Layer 4: the resulting node. At this layer, the node function calculates the contribution of all the i_{th} rules and transfers the summed contribution to the total output. The function can be written as follows:

$$O_{i4} = \bar{w}_i f_i = \bar{w}_i\left(p_i \times AD + q_i \times C + s_i \times \text{pH} + m_i \times T + g_i\right) \quad i = 1, 2 \tag{8}$$

where $\bar{w}_i$ denotes the Layer 3 output, whereby p_i, q_i, s_i, m_i and g_i are the parameter set. The parameters in this layer are stated as the consequent parameters.

Layer 5: the output node. This layer is the output layer. It calculates the total output by adding all the received indications. Therefore, a de-fuzzification procedure converts all the fuzzy rules outcomes into a crisp output.

$$O_{i5} = Q\sum_i \bar{w}_i f_i = \frac{\sum_i w_i f_i}{\sum_i w_i} \tag{9}$$

There is no limited rule designed for constructing the ANFIS system. However, a common context can be constructed based on earlier successful engineering applications. The ANFIS target is to specify and simplify the form relationship.

$$Y = f(X_1, X_2, \cdots, X_n) \tag{10}$$

where Y is the variable of output and X_1, X_2,..., X_n are the input variables.

In this paper, the removal capacity (Q) can be distinguished as the function of AD, C, PH and T. The input and the output (i.e., removal efficiency) relationship can be written as follows:

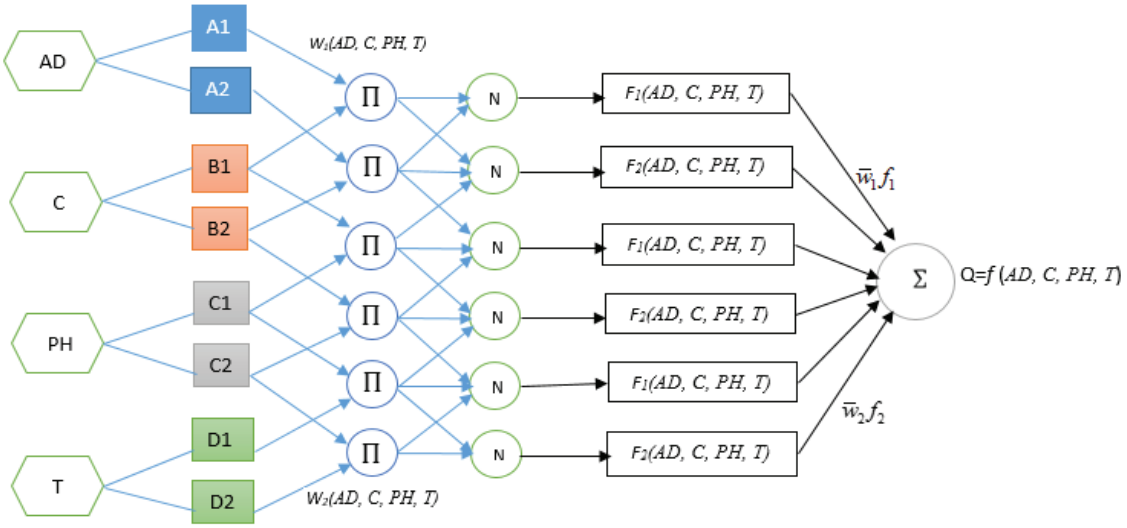

Fig. 2. Architecture of ANFIS.

$$Q = f(\mathrm{AD}, C, \mathrm{PH}, T) \quad (11)$$

The utilized data are divided into three sets. The first one is the training set. Most of the data are used in this section to train the ANFIS. The second set is a checking set and used to verify the defined ANFIS, which prevents over-fitting the network. The third set is the testing set, which is used to ascertain model accuracy and performance. In this study, 158 experimental results are used, which were divided as follows: 73% for training, 12% for checking and 15% for testing.

2.4. Model evaluation indicators

Two competing neural networks were developed. For the modeling in this study, the ANFIS and the FF-NN were used. An assessment of multi-criteria was performed. The performance of the ANFIS and FF-NN models was determined by comparing the actual data with the simulated dataset. The behavior of each model was examined employing the root mean square error (RMSE), relative error (RE), mean square error (MSE), relative root mean square error (RRMSE) and the mean absolute percentage error (MAPE). The formulas used to calculate these indicators are as follows:

$$\mathrm{MSE} = \frac{1}{n}\sum_{i=1}^{n}\left(D_{a(t)} - D_{f(t)}\right)^2 \quad (12)$$

$$\mathrm{RMSE} = \left[\frac{1}{n}\sum_{t=1}^{n}\left(D_{a(t)} - D_{f(t)}\right)^2\right]^{\frac{1}{2}} \quad (13)$$

$$\mathrm{RRMSE} = \left[\frac{1}{n}\sum_{t=1}^{n}\left(\frac{D_{a(t)} - D_{f(t)}}{D_{a(t)}}\right)^2\right]^{\frac{1}{2}} \quad (14)$$

$$\mathrm{MAPE} = \frac{1}{n}\sum\nolimits_{t=1}^{n}\left|\frac{\left(D_{a(t)} - D_{f(t)}\right)}{D_{a(t)}}\right| \times 100 \quad (15)$$

$$\mathrm{RE} = \frac{D_{a(t)} - D_{f(t)}}{D_{a(t)}} \times 100 \quad (16)$$

where $D_{a(t)}$ = the actual value. $D_{f(t)}$ = the simulated value.

Generally, MSE, RMSE, RE, MAPE and RRMSE equations were selected to indicate model performance, which was based on the result obtained by comparing the evaluated error of the actual and simulated results. The best model is considered the model with the smallest error.

3. Results and discussion

In this study, two modeling systems were used: the FF-NN and ANFIS systems. Various indicators were used to evaluate the two proposed methods. A comparison of the two methods was performed. Based on the comparison, the best model was adopted for a sensitivity study that used all the parameters involved in the experimental research: pH, adsorbent dosage and initial concentration. In addition, the adsorption rate was investigated using three kinetics models.

3.1. ANFIS vs. FF-NN performance

The feed-forward neural network (FF-NN) and the ANFIS modeling techniques presented in the methods section were used for the modeling in this study. "Accuracy" was defined as how closely a predicted value matches an actual value, whereas "precision" referred to how closely predicted values match one another. It was clear that the ANFIS model performed better than the FF-NN model according to the following indicators: MSE, RMSE, RRMSE and MAPE. The goal of the training section was to decrease the error function by creating a range of connection and initial values to help the network achieve an output nearly equal to the target values.

The FF-NN was trained using the Bayesian regularization (TRAINBR) algorithm, which is considered the fastest algorithm in the MATLAB toolbox and is recommended as the best choice for the supervised algorithm. Additionally, it does not require a large memory compared with other algorithms. The optimum neuron number in each hidden layer was recognized by trial and error by changing the number of neurons in the hidden layer from 2 to 20. Moreover, the number in the hidden layers of the model was identified by trial and error to determine the optimal network structure. The optimum model architecture was identified based on the minimum values of the MSE. Therefore, the optimal network structure contains four inputs, 15 neurons in each hidden layer with three hidden layers (Fig. 1), and one output. Fig. 3 compares the data obtained using the FF-NN with the experimental data. It shows a good compatibility between the experimental and predicted data.

Selecting the optimal network structure is the most significant problem in ANFIS training. The ANFIS structure consists of five layers (Fig. 2). The optimum architecture of the ANFIS system was identified based on the minimum values of testing-set error. Using the membership function for the input and linear type, which is applied for the output while generating the FIS, the optimal method was identified. As presented in Table 1, the minimum testing error obtained for the ANFIS model was 6.14×10^{-5} (MSE). Consequently, the ANFIS model system with a linear output MF type, three MFs for the input, "bellmf" as MF type and 100 epochs was

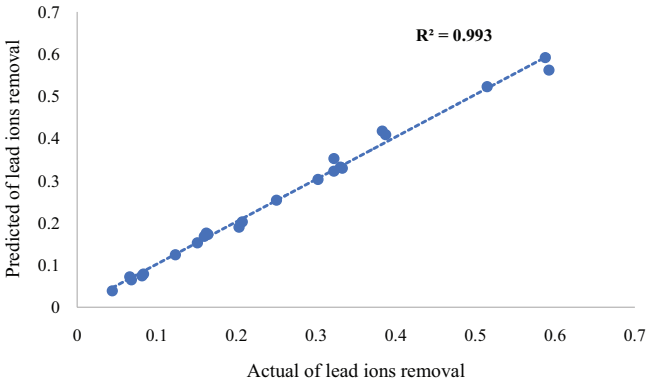

Fig. 3. R^2 of ANN.

designated the optimal model structure. To verify its accuracy, the ANFIS model was used to simulate 22 results, which were not used in the training or validation procedures. The comparison between the actual and predicted data is presented in Fig. 4. The determination coefficient for the testing dataset R^2 is 0.9981, which indicates a superior performance of ANFIS model compared with the FF-NN model. The data scatter is nearly along a 45° line, which indicates the superior performance of the ANFIS model.

Regarding the MSE values for the ANFIS and FF-NN models (Table 1), the MSE of ANFIS was 6.14×10^{-5}. This outcome is a practical value and reflects accuracy and high efficacy compared with the MSE of the FF-NN, which was 1.86×10^{-4}. The ANFIS model can be used to simulate the connection between the input variables and thus to investigate the adsorbent capacity of a functionalized carbon nanotube. The MAPE value for the ANFIS model was 2.02%. In contrast, the MAPE value for the FF-NN model was 4.53%. This outcome demonstrates that the ANFIS model is more accurate than the FF-NN model. Additionally, the ANFIS model produced RMSE and RRMSE values of 6.47×10^{-3} and 5.91×10^{-3}, respectively, whereas the FF-NN results were 1.36×10^{-2} and 5.74×10^{-2}, respectively. Consequently, these criteria confirm that the ANFIS model performed better than the FF-NN model.

Relative error is an error indicator in modeling prediction. It compares actual values to predicted values. Fig. 5 shows the relative error percentages for the ANFIS and FF-NN models. A total of 22 results were used for both models to test their accuracy. The maximum error value for the FF-NN model was 11.62% as opposed to 7.07% for the ANFIS model. The results were calculated using Eq. (16) and indicate that the ANFIS model is more accurate than the FF-NN model.

This outcome demonstrates the reliability and effectiveness of the proposed approach to extracting features from input data. The hybrid ANFIS model can provide perfect prediction of KTEG-CNTs as a Pb(II) absorber from water. The ANFIS model was used for the sensitivity analysis.

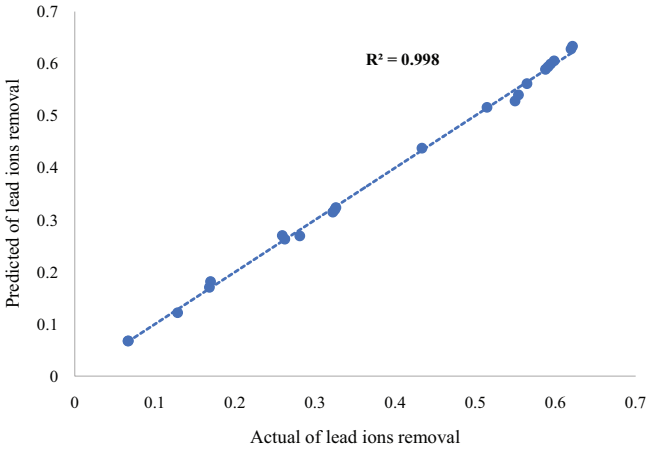

Fig. 4. R^2 of ANFIS.

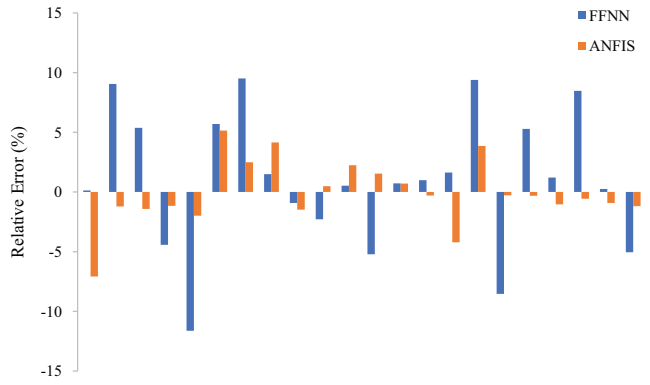

Fig. 5. Illustration of the accuracy of the hybrid model.

3.2. Sensitivity analysis

3.2.1. pH study

pH is one of the most influential factors in the adsorption process. It affects the interactions between the adsorbent surface and Pb(II). In addition, pH influences the quantity and form of the adsorbent surface active sites. It also affects the solubility of metals ions in solution [33]. Here, the effect of pH on the adsorption process is determined using 12.5 mg of adsorbent dosage to remove 5 mg/L of Pb(II) from contaminated water at 5 min contact time. The pH value ranged from 1 to 10. Based on the results shown in Fig. 6, by increasing the pH values, the adsorption capacity increases due to the reduction of positive ions competition. At pH 5 the reduction of positive charged competitive ions will be at the maximum level and the free negative active sites on the adsorbent surface becomes totally free to receive the heavy metals ions only. Additionally, by increasing the pH to 6, the adsorption capacity remains nearly steady.

At a pH higher than 7.0, the adsorption capacity is increased when the dominant species of Pb(II) ions are $Pb(OH)^+$ and $Pb(OH)_2$. This complexation might be caused by the extensive presence of OH^- at this pH level, which results in precipitation [34]. Moreover, with increasing the pH of the water solution, the presence of H^+ decreases due to the extensive presence of OH^-, which plays a significant role in decreasing the H^+ of the solution. As a result, the competition on the adsorbent active sites decreases, and the adsorption capacity increases. The agreement of the ANFIS model predictions as a function of pH is presented in Fig. 6. It can be noted that the results obtained using the proposed

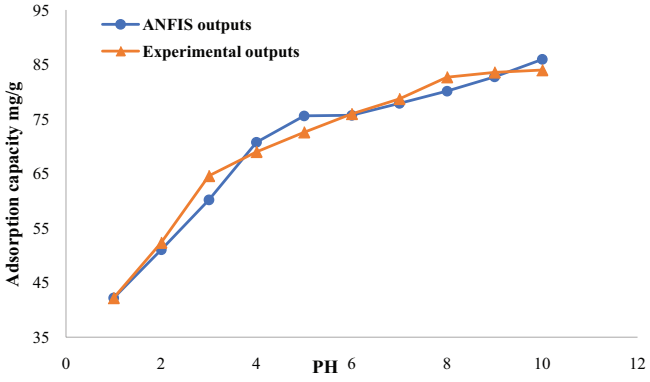

Fig. 6. Agreement between ANFIS outputs and experimental outputs with various pH values.

ANFIS model indicate nearly the same behavior as the experimental data. This outcome demonstrates the accuracy of the proposed model.

3.2.2. Initial concentration study

The effect of the initial concentration on the adsorption capacity was investigated by varying the initial concentration of lead from (from 5 to 60 mg/L). The initial concentration effect was examined at 2.7 pH, a 15-min contact time and a 5-mg adsorbent dosage. The initial concentration of lead increased from 5 to 10 mg/L, and the uptake capacity increased from 32.48 to 49.57 mg/g, whereas by increasing the initial concentration from 10 to 20 mg/L, the uptake capacity increased from 49.75 to 101.05 mg/g. This outcome might be attributed to the increase in the driving force of the mass transfer, which resulted in an increase in the quantity of Pb(II) adsorbed from water solution. At low concentration, Pb(II) interacts at the adsorbent active sites, whereas at a higher Pb(II) concentration, the adsorbent active sites are saturated, and the removal percentage is lower [35]. The data obtained from the experimental research were trained and predicted using ANFIS modeling. The ANFIS model prediction was found satisfactory for the experimental data. The experimental and predicted outputs of the ANFIS are presented in Fig. 7.

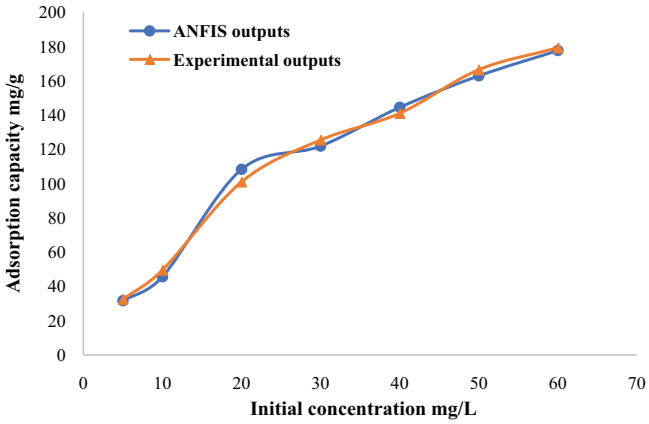

Fig. 7. Experimental and ANFIS output as the function of initial concentration.

3.2.3. Adsorbent dosage study

Adsorbent dosage is an important factor involved in the adsorption process. The effect of the adsorbent dosage on Pb(II) removal was examined at pH 3.0, an initial concentration of 20 mg/L of Pb(II) and a contact time of 15 min. The KTEG-CNTs adsorption capacity decreased from 123.94 to 76.292 mg/g when the adsorbent dosage was increased from 5 to 12.5 mg. It decreased from 44.425 to 23.584 mg/g when the adsorbent dosage was increased from 20 to 30 mg. The decrease in the uptake capacity accompanied by the increase in the adsorbent dosage might be attributed to increasing the adsorbent surface area following an increase in the number of active sites [36]. The data obtained from the experiment were trained and predicted using the ANFIS model. The ANFIS model prediction was found satisfactory for the experimental data. The experimental and predicted output of the ANFIS are presented in Fig. 8.

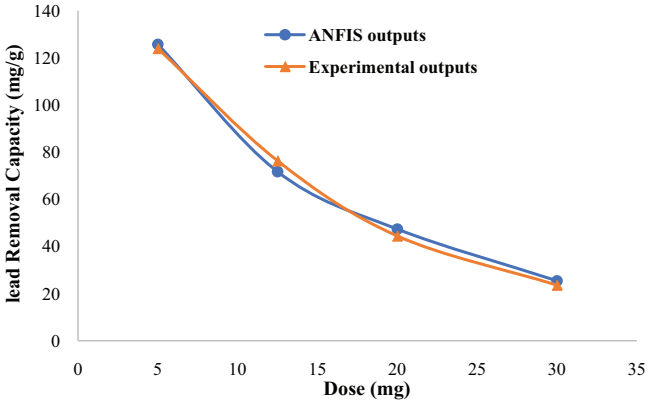

Fig. 8. Experimental and ANFIS output as the function of adsorbent dosage.

3.2.4. Adsorption kinetics study

It is important to determine the kinetics of the adsorption reaction rates of any adsorption system. In this study, three kinetic models were used (i.e., pseudo-first-order, pseudo-second-order and intraparticle diffusion models) to investigate the mechanism and rate of the adsorption process. The kinetic study was performed at three initial concentration (C_0 mg/L) values of 8, 12 and 18 mg/L and an adsorbent dosage of 5 mg. pH and contact time were regarded as variable. pH is one of the most influential factors in the adsorption process. Therefore, three pH values were used: 2.7, 6 and 8.

The adsorption kinetics for lead ion removal from water by KTEG-CNTs was studied applying the proposed ANFIS model to determine the adsorption rate and to confirm the accuracy and usability of the proposed ANFIS model. Table 2 presents the results for the three models that were used. The correlation coefficient (R^2) for the pseudo-first-order model was in the range of 0.226 to 0.972. However, for the pseudo-second-order model, it was in the range of 0.990 to 0.999, and for the intraparticle diffusion model, it was in the range of 0.861 to 0.994. Based on these results, the adsorption data were described well by the pseudo-second-order model. The model outcome for the simulated data resembles the model outcome for the experimental data [25]. Figs. 9(a)–(c) show the pseudo-second-order kinetic model with different values of pH and initial concentration. It is obvious from Fig. 9 that by increasing the initial concentration of Pb(II) the value of (t/q) is decreased. That is, the metal uptake capacity is proportional to the initial concentration, which is the driving force for mass transfer [37].

4. Conclusion

FF-NN and ANFIS techniques were successfully used to predict the removal of Pb(II) from an aqueous solution using DES-functionalized CNTs. The effect of various pH values on the adsorption of lead ions from water was investigated. A kinetic study was performed using different values of initial concentration and various pH values. Three different

Table 2
Adsorption kinetics and correlation coefficient

		Pseudo-first-order $\ln(q_e - q_t)$ vs. time (t)	Pseudo-second-order $(t/q_t$ vs. $t)$	Intraparticle $(q_t$ vs. $t^{0.5})$
PH	C_0 mg/L	R^2	R^2	R^2
2.7	8	0.972	0.998	0.861
2.7	12	0.226	0.990	0.956
2.7	18	0.679	0.991	0.951
6	8	0.524	0.995	0.982
6	12	0.946	0.998	0.994
6	18	0.888	0.999	0.986
8	8	0.433	0.997	0.861
8	12	0.753	0.999	0.956
8	18	0.707	0.999	0.951

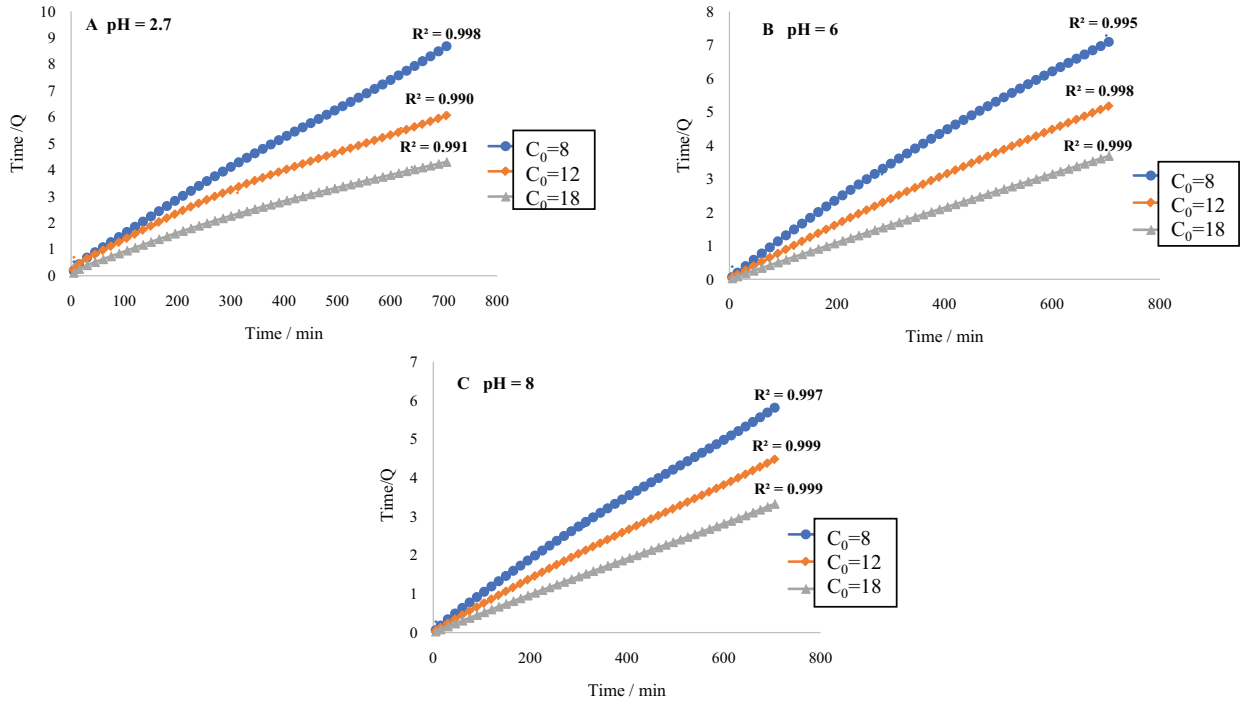

Fig. 9. Pseudo-second-order adsorption kinetics at different pH and initial concentrations.

kinetic models were used to study the adsorption reaction rate. The pseudo-second-order kinetic model described the adsorption data sufficiently. The development of the two systems was such that we could obtain the optimal topology of both models during the training section. The models were created with the same purpose and their performance was compared. The performance of the ANFIS model was better than that of the FF-NN model in terms of accuracy. The ANFIS model was found to perform excellently in the prediction of the adsorption capacity of lead ions.

The prediction value of the ANFIS model was close to the real values: $R^2 = 0.998$, MSE = 6.14×10^{-5}, RMSE = 6.47×10^{-3}, RRMSE = 5.91×10^{-3} and MAPE = 2.02. This outcome indicates that the ANFIS system can model the adsorption capacity of lead ions using DES-functionalized CNTs. One benefit of the proposed modeling technique is its simplification of the process used by researchers to recognize the significant effect of each parameter involved in removal efficiency.

Acknowledgment

The authors express their thanks to the University of Malaya for funding this research. UMRG (RP025C-18SUS).

References

[1] D.I. Mendoza-Castillo, C.K. Rojas-Mayorga, I.P. García-Martínez, M.A. Pérez-Cruz, V. Hernández-Montoya, A. Bonilla-Petriciolet, M.A. Montes-Morán, Removal of heavy metals and arsenic from aqueous solution using textile wastes from denim industry, Int. J. Environ. Sci. Technol., 12 (2015) 1657–1668.

[2] D.G. Mazumder, B. Mandal, T. Chowdhury, G. Samanta, G. Basu, P. Chowdhury, C. Chanda, D. Lodh, D. Chakraborti, Chronic arsenic toxicity in West Bengal, Curr. Sci., 72 (1997) 114–117.

[3] T. Bahadir, G. Bakan, L. Altas, H. Buyukgungor, The investigation of lead removal by biosorption: an application at storage battery industry wastewaters, Enzyme Microb. Technol., 41 (2007) 98–102.

[4] M. Bissen, F.H. Frimmel, Arsenic — a review. Part II: Oxidation of arsenic and its removal in water treatment, Acta Hydrochim. Hydrobiol., 31 (2003) 97–107.
[5] R.Y. Ning, Arsenic removal by reverse osmosis. Desalination, 143 (2002) 237–241.
[6] P. Ratna Kumar, S. Chaudhari, K.C. Khilar, S.P. Mahajan, Removal of arsenic from water by electrocoagulation, Chemosphere, 55 (2004) 1245–1252.
[7] T.M. Gihring, G.K. Druschel, R.B. McCleskey, R.J. Hamers, J.F. Banfield, Rapid arsenite oxidation by *Thermus aquaticus* and *Thermus thermophilus*: field and laboratory investigations, Environ. Sci. Technol., 35 (2001) 3857–3862.
[8] J. Kim, M.M. Benjamin, Modeling a novel ion exchange process for arsenic and nitrate removal, Water Res., 38 (2004) 2053–2062.
[9] S. Ye, G. Zeng, H. Wu, C. Zhang, J. Dai, J. Liang, J. Yu, X. Ren, H. Yi, M. Cheng, C. Zhang, Biological technologies for the remediation of co-contaminated soil, Crit. Rev. Biotechnol., 37 (2017) 1062–1076.
[10] S. Ye, G. Zeng, H. Wu, C. Zhang, J. Liang, J. Dai, Z. Liu, W. Xiong, J. Wan, P. Xu,. M. Cheng, Co-occurrence and interactions of pollutants, and their impacts on soil remediation—a review, Crit. Rev. Environ. Sci. Technol., 47 (2017) 1528–1553.
[11] H. Wu, C. Lai, G. Zeng, J. Liang, J. Chen, J. Xu, J. Dai, X. Li, J. Liu, M. Chen, L. Lu, L. Hu, J. Wan, The interactions of composting and biochar and their implications for soil amendment and pollution remediation: a review, Crit. Rev. Biotechnol., 37 (2017) 754–764.
[12] E. Lourie, E. Gjengedal, Metal sorption by peat and algae treated peat: kinetics and factors affecting the process, Chemosphere, 85 (2011) 759–764.
[13] J.P. Chen, Wu, Acid/base-treated activated carbons: characterization of functional groups and metal adsorptive properties, Langmuir, 20 (2004) 2233–2242.
[14] J.U.K. Oubagaranadin, Z.V.P. Murthy, Isotherm modeling and batch adsorber design for the adsorption of Cu(II) on a clay containing montmorillonite, Appl. Clay Sci., 50 (2010) 409–413.
[15] V.K. Gupta, A. Rastogi, V.K. Saini, N. Jain, Biosorption of copper(II) from aqueous solutions by Spirogyra species, J. Colloid Interface Sci., 296 (2006) 59–63.
[16] K. Yetilmezsoy, S. Demirel, Artificial neural network (ANN) approach for modeling of Pb(II) adsorption from aqueous solution by Antep pistachio (*Pistacia Vera* L.) shells, J. Hazard. Mater., 153 (2008) 1288–1300.
[17] R.K. Ibrahim, M. Hayyan, M.A. AlSaadi, A. Hayyan, S. Ibrahim, Environmental application of nanotechnology: air, soil, and water, Environ. Sci. Pollut. Res., 23 (2016) 13754–13788.
[18] Ihsanullah, A. Abbas, A.M. Al-Amer, T. Laoui, M.J. Al-Marri, M.S. Nasser, M. Khraisheh, M.A. Atieh, Heavy metal removal from aqueous solution by advanced carbon nanotubes: critical review of adsorption applications, Sep. Purif. Technol., 157 (2016) 141–161.
[19] M.K. AlOmar, M.A. Alsaadi, M. Hayyan, S. Akib, M.A. Hashim, Functionalization of CNTs surface with phosphonuim based deep eutectic solvents for arsenic removal from water, Appl. Surf. Sci., 389 (2016) 216–226.
[20] A.P. Abbott, G. Capper, D.L. Davies, R.K. Rasheed, V. Tambyrajah, Novel solvent properties of choline chloride/urea mixtures, Chem. Commun., 9 (2003) 70–71.
[21] M.K. AlOmar, M. Hayyan, M.A. Alsaadi, S. Akib, A. Hayyan, M.A. Hashim, Glycerol-based deep eutectic solvents: physical properties, J. Mol. Liq., 215 (2016) 98–103.
[22] A,P. Abbott, K. El Ttaib, G. Frisch, K.J. McKenzie, K.S. Ryder, Electrodeposition of copper composites from deep eutectic solvents based on choline chloride, Phys. Chem. Chem. Phys., 11 (2009) 4269–4277.
[23] M.K. AlOmar, M.A. Alsaadi, M. Hayyan, S. Akib, M. Ibrahim, M.A. Hashim, Allyl triphenyl phosphonium bromide based DES-functionalized carbon nanotubes for the removal of mercury from water, Chemosphere, 167 (2017) 44–52.
[24] A.P. Abbott, D. Boothby, G. Capper, D.L. Davies, R.K. Rasheed, Deep eutectic solvents formed between choline chloride and carboxylic acids: versatile alternatives to ionic liquids, J. Am. Chem. Soc., 126 (2004) 9142–9147.
[25] M.K. AlOmar, M.A. Alsaadi, M. Hayyan, S. Akib, R.K. Ibrahim, M.A. Hashim, Lead removal from water by choline chloride based deep eutectic solvents functionalized carbon nanotubes, J. Mol. Liq., 222 (2016) 883–894.
[26] S. Mandal, P.V. Sivaprasad, S. Venugopal, K.P.N. Murthy, Artificial neural network modeling to evaluate and predict the deformation behavior of stainless steel type AISI 304L during hot torsion, Appl. Soft Comput., 9 (2009) 237–244.
[27] O.K. Chibole, Modeling River Sosiani's water quality to assess human impact on water resources at the catchment scale, Ecohydrol. Hydrobiol., 13 (2013) 241–245.
[28] A.H. El-Shafie, M.S. El-Manadely, An integrated neural network stochastic dynamic programming model for optimizing the operation policy of Aswan High Dam, Hydrol. Res., 42 (2011) 50–67.
[29] A. El-Shafie, M.R. Taha, A. Noureldin, A neuro-fuzzy model for inflow forecasting of the Nile river at Aswan high dam, Water Resour. Manage., 21 (2007) 533–556.
[30] E.H. Mamdani, S. Assilian, An experiment in linguistic synthesis with a fuzzy logic controller, Int. J. Man. Mach. Stud., 7 (1975) 1–13.
[31] T. Takagi, M. Sugeno, Fuzzy identification of systems and its applications to modeling and control, IEEE Trans. Syst. Man Cybern., SMC-15 (1985) 116–132.
[32] J.-S.R. Jang, C.-T. Sun, E. Mizutani, Neuro-fuzzy and soft computing; a computational approach to learning and machine intelligence, 1997.
[33] A. Salisu, M.M. Sanagi, A. Abu Naim, W.A. Wan Ibrahim, K.J. Abd Karim, Removal of lead ions from aqueous solutions using sodium alginate-graft-poly(methyl methacrylate) beads, Desal. Wat. Treat., 57 (2016) 15353–15361.
[34] V.K. Gupta, S. Agarwal, T.A. Saleh, Synthesis and characterization of alumina-coated carbon nanotubes and their application for lead removal, J. Hazard. Mater., 185 (2011) 17–23.
[35] A. Banerjee, P. Sarkar, S. Banerjee, Application of statistical design of experiments for optimization of As (V) biosorption by immobilized bacterial biomass, Ecol. Eng., 86 (2016) 13–23.
[36] B. Das, N. Mondal, R. Bhaumik, P. Roy, Insight into adsorption equilibrium, kinetics and thermodynamics of lead onto alluvial soil, Int. J. Environ. Sci. Technol., 11 (2014)1101–1114.
[37] P. Geetha, M.S. Latha, S.S. Pillai, M. Koshy, Nanoalginate based biosorbent for the removal of lead ions from aqueous solutions: equilibrium and kinetic studies, Ecotoxicol. Environ. Saf., 122 (2015) 17–23.